Article

Synthesis, Characterization, and Cytotoxicity of New Spirooxindoles Engrafted Furan Structural Motif as a Potential Anticancer Agent

Mezna Saleh Altowyan,* Saied M. Soliman, Matti Haukka, Nora Hamad Al-Shaalan, Aminah A. Alkharboush, and Assem Barakat*

Read Online

ACCESS | 📊 Metrics & More | 📖 Article Recommendations | 🆂🅸 Supporting Information

3b
IC$_{50}$ = 4.1±0.1μM (MCF-7)
IC$_{50}$ = 3.5±0.07μM (HepG2)
STD (Staurosporine)
IC$_{50}$ = 17.8±0.50 μM (MCF-7)
IC$_{50}$ = 10.3±0.23 μM (HepG2)

3d
IC$_{50}$ = 4.3±0.18 μM (MCF-7)
STD (Staurosporine)
IC$_{50}$ = 17.8±0.50 μM (MCF-7)

3f
IC$_{50}$ = 3.5±0.11 μM (HepG2)
STD (Staurosporine)
IC$_{50}$ = 10.3±0.23 μM (HepG2)
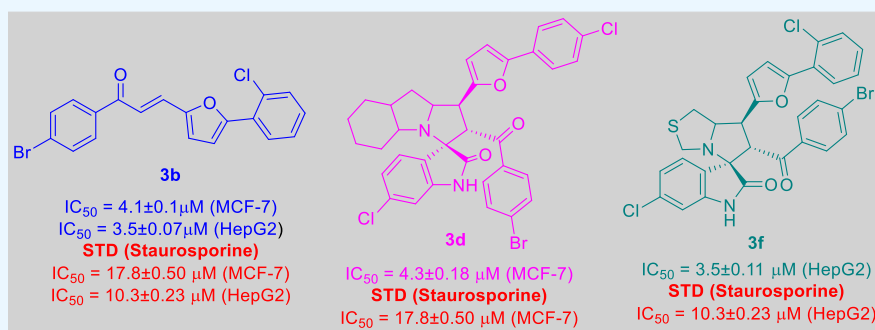
ABSTRACT: A new series of spirooxindoles based on ethylene derivatives having furan aryl moiety are reported. The new hybrids were achieved via [3 + 2] cycloaddition reaction as an economic one-step efficient approach. The final constructed spirooxindoles have four contiguous asymmetric carbon centers. The structure of **3a** is exclusively confirmed using X-ray single crystal diffraction. The supramolecular structure of **3a** is controlled by O···H, H···H, and C···C intermolecular contacts. It includes layered molecules interconnected weak C−H···O (2.675 Å), H···H (2.269 Å), and relatively short Cl···Br interhalogen interactions [3.4500(11)Å]. Using Hirshfeld analysis, the percentages of these intermolecular contacts are 10.6, 25.7, 6.4, and 6.2%, respectively. The spirooxindoles along with ethylene derivatives having furan aryl moiety were assessed against breast (MCF7) and liver (HepG2) cancer cell lines. The results indicated that the new chalcone **3b** showed excellent activity in both cell lines (MCF7 and HepG2) with IC$_{50}$ = 4.1 ± 0.10 μM/mL (MCF7) and 3.5 ± 0.07 μM/mL (HepG2) compared to staurosporine with 4.3 and 2.92 folds. Spirooxindoles **6d** (IC$_{50}$ = 4.3 ± 0.18 μM/mL), **6f** (IC$_{50}$ = 10.3 ± 0.40 μM/mL), **6i** (IC$_{50}$ = 10.7 ± 0.38 μM/mL), and **6j** (IC$_{50}$ = 4.7 ± 0.18 μM/mL) exhibited potential activity against breast adenocarcinoma, while compounds **6d** (IC$_{50}$ = 6.9 ± 0.23 μM/mL) and **6f** (IC$_{50}$ = 3.5 ± 0.11 μM/mL) were the most active hybrids against human liver cancer cell line (HepG2) compared to staurosporine [IC$_{50}$ = 17.8 ± 0.50 μM/mL (MCF7) and 10.3 ± 0.23 μM/mL (HepG2)]. Molecular docking study exhibited the virtual mechanism of binding of compound **3b** as a dual inhibitor of EGFR/CDK-2 proteins, and this may highlight the molecular targets for its cytotoxic activity.

1. INTRODUCTION

In the last decade, spirooxindole scaffold has been recognized as a potential pharmacophore in drug discovery, particularly for cancer research development.[1−3] Spirooxindole has a unique rigid structural architecture with the diversity of pharmaceutical activities which made this nucleus a privileged structure in the new drug discovery. The exploration and discovery of novel drugs for anticancer therapy with lower toxicity and high selectivity is always an area of intensive research. Many examples having spirooxindoles have been reported so far for cancer therapy research and exhibited durable regression for cancer treatment with oral administration in the preclinical advanced stages; as an example MI-888 is a lead compound having spiro-pyrrolidinyl oxindole for p53-MDM2 protein−protein interaction inhibitors.[4] MI-773 and MI-219 are other two representative examples having spirooxindole-pyrrolidine

derivatives which exhibited cytotoxicity and interfered with the proteasomal degradation of p53.[5,6]

Several structural pharmacophores have been coadministrated with the spirooxindole privileged structures inspired by research for structural complexities with their diverse bioactivities.[7,8] Due to the urgent need to discover a new cancer agent with more targeting to cancer cells and less harmful for the normal tissue, chemists have synthesized many
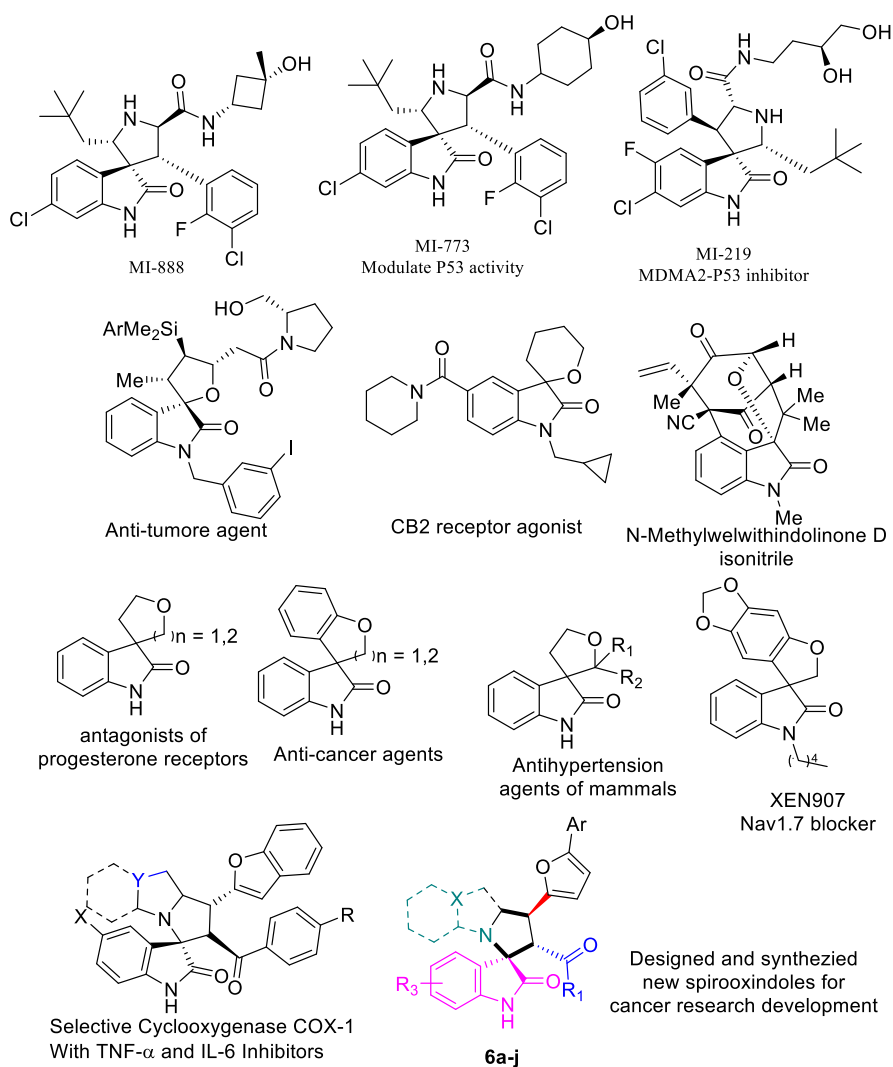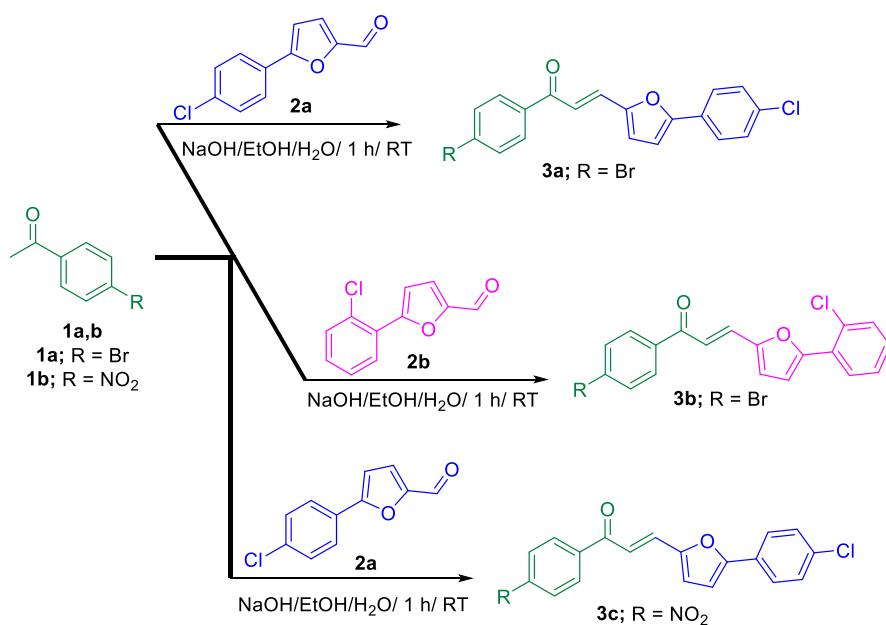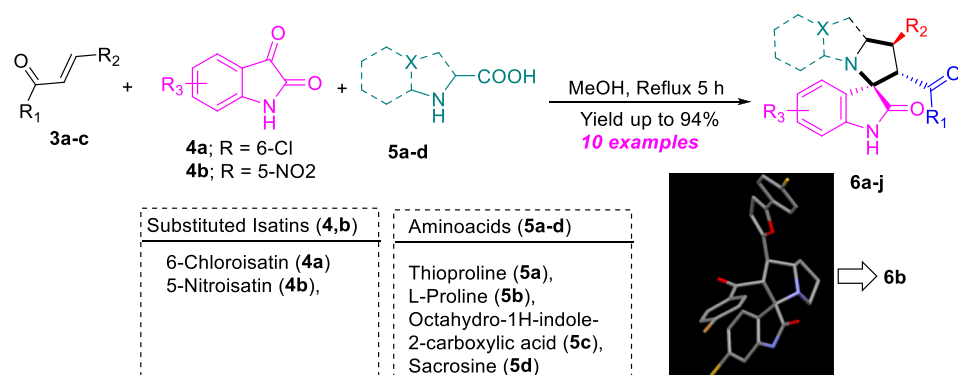
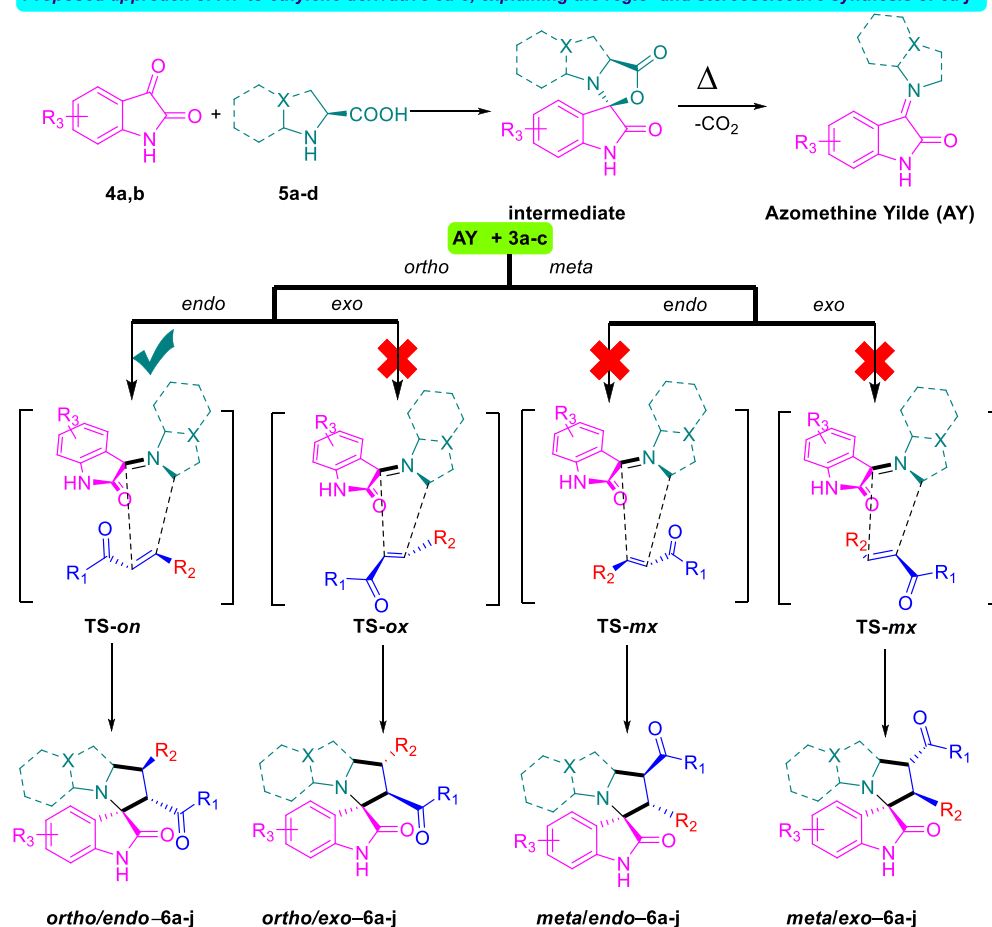**Figure 1.** Some biologically active spirooxindole-based pharmacophores.

Scheme 1. Synthetic Route for the Ethylene Derivatives 3a−c Engrafted Aryl-Furan Ring

Scheme 2. A Plausible Mechanism for the 32CA Reaction of Azomethine Ylide to Ethylene Derivative 3a−c to Afford the Spirooxindole Analogues 6a−j

spirooxindoles for this purpose. In particular, spirooxindoles containing furan scaffold, which are called oxa-spirooxindoles, widely exist in many natural and biologically active molecules.[8−15] The designed, synthesized, and reported spirooxindoles show anticancer activity and can serve as an anti-tumor agent, CB2 receptor agonist, antagonists of progesterone receptors, antagonists of progesterone receptors, Nav1.7 blocker (XEN907), and selective cyclooxygenase COX-1 with TNF-α and IL-6 Inhibitors.[16−19]

Spirooxindole core has been continuously attracting the attention of researchers and has become a dynamic area of research due to its outstanding pharmacological properties.

Barakat et al. extensively studied this spirooxindole scaffold recently and have reported so many examples so far focusing on the drug discovery research.[20−28] In this library, Barakat has reported the synthesis of a new class of new spiro-heterocycles coadministrated with different pharmacophores such thiochromene, benzofuran, benzothiophene, cyclohexanone, pyrrole, and rhodanine scaffolds by the three-component [3 + 2] cycloaddition reaction in a regio- and stereo-selective fashion. All synthesized compounds were subjected to anticancer activity against a variety of cancer cell lines such as PC3, HeLa, MCF-7, MDA-MB231, and so forth, and many of them showed high efficacy against the tested cell lines.
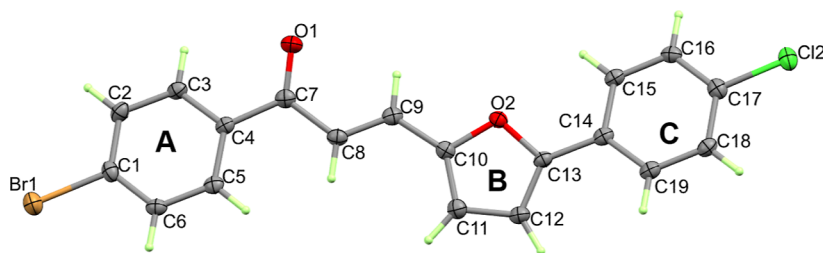
Figure 2. Thermal ellipsoids at 30% probability level showing atom numbering of **3a**.

Based on these findings and in continuation of our research program toward the synthesis of multifunctionalized spirooxindole drug skeleton for drug research development, we report here the new spirooxindole system appending the furan structural pharmacophore. The molecular features of the new spirooxindole derivative compound were elucidated based on X-ray diffraction of a single crystal, Hirshfeld analysis, and atoms-in-molecules calculations. Also, the spirooxindoles along with ethylene derivatives having the aryl-furan moiety were assessed against two cancer cell lines including breast adenocarcinoma (MCF7) and liver cancer cell line (HepG2) (Figure 1).

2. RESULTS AND DISCUSSION

2.1. Chemistry. New spirooxindoles having aryl-furan motif were designed and synthesized according to Scheme 1. The ethylene derivatives **3a–c** having the aryl-furan scaffold was mandatory as a dipolarphile for the [3 + 2] cycloaddition reaction approach and were prepared from the acetophenones with the aryl-furan carbaldehydes in basic condition to afford the corresponding chalcones in precipitated form in a high chemical yield. The ethylene derivative **3a** was successfully obtained in a single crystalline form by slow diffusion/ evaporation in DCM/EtOH, and the crystal was suitable for X-ray diffraction analysis. The required materials for the [3 + 2] cycloaddition reaction were ethylene derivative having aryl-furan motif **3a–c**, four amino acids **5a–d**, and two substituted isatins **4a,b**, which achieved the desired spirooxindoles **6a–j**. Ten examples were successfully synthesized in stereoselective and high chemical yield up to 94%. A set of trials were carried out to get any of those final compounds in a crystalline form and only one compound (**6b**) was provided as crystal; it was not good enough to provide the optimum X-ray data for publication quality but at least gave us the main skeleton of the final compound. Other spectrophotometric tools were employed to prove the chemical structure. The plausible mechanism is depicted in Scheme 2 based on the previous reported literature.[29−33]

2.2. Crystal Structure Description of 3a. The X-ray structure of **3a** is shown in Figure 2 which is found in good agreement with its spectral characterizations. Compound **3a** crystallized in the monoclinic crystal system and the $P2_1/c$ space group with z = 4 and one molecular unit as asymmetric formula (Table 1). The unit cell parameters are a = 19.4870(9) Å, b = 13.8512(6) Å, c = 5.8412(3) Å, β = 92.720(6)°, and V = 1574.87(13) Å³. The list of bond distances and angles is given in Table 2. The structure comprised three aromatic planar ring systems. These rings are abbreviated **A**, **B**, and **C** for simplicity (Figure 2). It is worth to note that the three rings are twisted with one another to different extents. The mean plane of ring **A** is found twisted

Table 1. Crystal Data

	3a
CCDC	2165902
empirical formula	$C_{19}H_{12}BrClO_2$
f_w	387.65
temp (K)	120(2)
λ (Å)	0.71073
cryst syst.	monoclinic
space group	$P2_1/c$
a (Å)	19.4870(9)
b (Å)	13.8512(6)
c (Å)	5.8412(3)
β (deg)	92.720(6)
V (Å³)	1574.87(13)
Z	4
ρ_{calc} (Mg/m³)	1.635
μ (Mo Kα) (mm^{-1})	2.786
no. reflns.	14253
unique reflns.	3887
completeness to θ = 25.242°	99.8%
GOOF (F^2)	1.065
R_{int}	0.0558
$R_1{}^a$ ($I \geq 2\sigma$)	0.0547
$wR_2{}^b$ ($I \geq 2\sigma$)	0.1134

$^a R_1 = \Sigma||F_o| - |F_c||/\Sigma|F_o|$. $^b wR_2 = \{\Sigma[w(F_o{}^2 - F_c{}^2)^2]/\Sigma[w(F_o{}^2)^2]\}^{1/2}$.

Table 2. Selected Bond Lengths [Å] and Angles [deg] for 3a

atoms	distance	atoms	distance
Br(1)−C(1)	1.889(4)	O(2)−C(13)	1.368(4)
Cl(2)−C(17)	1.732(4)	O(2)−C(10)	1.380(4)
O(1)−C(7)	1.234(4)		

atoms	angle	atoms	angle
C(13)−O(2)−C(10)	107.3(3)	C(2)−C(1)−Br(1)	120.2(3)
C(6)−C(1)−C(2)	121.0(4)	C(3)−C(2)−C(1)	118.3(4)
C(6)−C(1)−Br(1)	118.8(3)		

with respect to ring **B** by 12.95°. The corresponding values for ring **C** is 8.8° with respect to the mean plane of ring **B**.

The supramolecular structure of **3a** is controlled by different types of intermolecular contacts (Figure 3). The most important contacts are emphasized by different colors in the packing scheme shown in Figure 4. H⋯O (magenta), H⋯H (purple), C⋯C (orange), and Br⋯Cl (turquoise) are the main contacts in this crystal structure. The presence of short Br⋯Cl (3.450 Å) and C⋯C (C8vC15; 3.323 Å and C9⋯C13; 3.399 Å) contacts revealed the presence of significant interhalogen and π−π stacking interactions, respectively. The rest of the interactions are O⋯H and H⋯H and are depicted in Table 3.

2.3. Hirshfeld Surface Analysis. Crystal structure stability is governed by intermolecular interactions among different
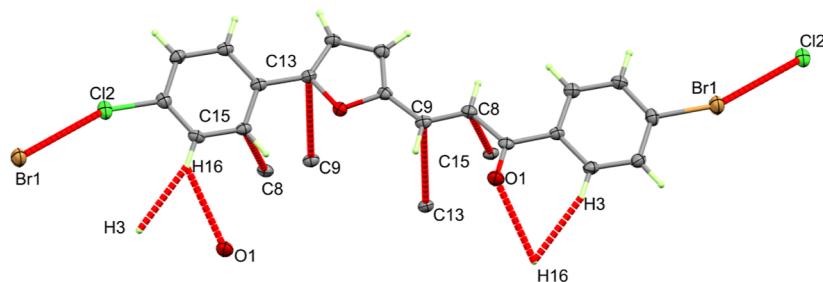
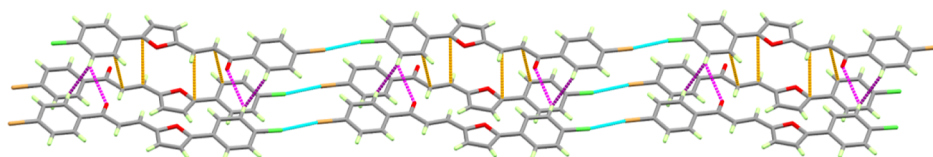**Figure 3.** Most important intermolecular contacts in the crystal structure of **3a**.

Figure 4. Packing of the molecular units via H⋯O (magenta), H⋯H (purple), C⋯C (orange), and Br⋯Cl (turquoise) in **3a**.

Table 3. Different Contacts and Their Distances (Å)

contact	distance	symm. code
Br1⋯Cl2	3.4500(11)	$-1 + x, y, -1 + z$
C8⋯C15	3.323(4)	$1 - x, 1 - y, 1 - z$
C9⋯C13	3.399(4)	$1 - x, 1 - y, 1 - z$
O1⋯H16	2.675	$1 - x, 1 - y, 2 - z$
H3⋯H16	2.269	$1 - x, 1 - y, 2 - z$

fragments in the crystal. Hirshfeld analysis is a simple tool for decomposition of different intermolecular contacts in the crystal. Different Hirshfeld surfaces including d_{norm}, shape index, and curvedness maps are shown in Figure 5. The d_{norm}
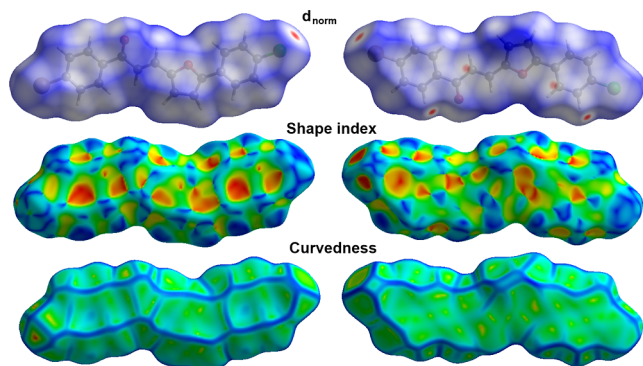
Figure 6. Intermolecular contacts and their percentages in **3a**.

Figure 5. Hirshfeld surfaces of **3a**.

map contains a number of red spots which represent the regions at which the important and short distance contacts occurred. Summary of all contacts and their percentages based on Hirshfeld calculations is presented in Figure 6.

Analysis of these interactions using fingerprint plot and d_{norm} maps is given in Figure 7. The major contacts are H⋯H, H⋯C, and O⋯H interactions, and their percentages are 25.7, 27.6, and 10.6%, respectively. It is worth noting that the red spots shown in the d_{norm} map are related to the Br⋯Cl (6.2%), C⋯C (6.4%), and H⋯H contacts. Hence, the hydrogen–hydrogen interactions are not only the most common but also considered strong. The H3⋯H16 contact (2.06 Å) is the shortest of these interactions. Also, the presence of short Br1⋯Cl2 (3.45 Å) revealed the presence of interhalogen
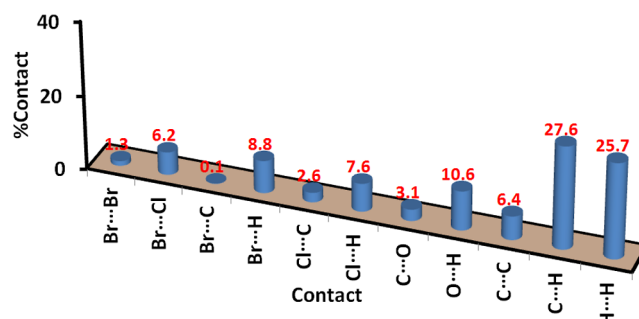
interactions, whereas the short C13⋯C9 (3.399 Å) and C16⋯C9 (3.323 Å) contacts revealed the importance of the π−π stacking interactions. The latter is further confirmed by the presence of red/blue triangles in the shape index map (Figure 5). The O1⋯H16 contact appeared as a blue region in the d_{norm} map. The corresponding interaction distance is found to be 2.674 Å based on Hirshfeld analysis. This value is slightly greater than the vdWs radii sum (2.61 Å) of the O and H atoms. Other contacts shown in this figure are considered weak interactions and have less contribution in the molecular packing of **3a**.

2.4. Biological Activity of the Synthesized Compounds. The ethylene derivatives having the aryl-furan moiety and the spirooxindoles were assessed against two cancer cell lines including breast and liver carcinoma by the MTT assay. Interestingly, the new chalcone **3b** discovered is the most active member between the synthesized compounds against both cell lines, with IC$_{50}$ = 4.1 ± 0.10 and 3.5 ± 0.07 μM/mL for MCF7 and HepG2, respectively, and more potent than the standard drug used as staurosporine [IC$_{50}$ = 17.8 ± 0.50 μM/mL (MCF7) and 10.3 ± 0.23 μM/mL (HepG2)]. The other two chalcones **3a** and **3c** show moderate activity (Table 4).

Although compounds **3a** and **3b** are two isomers with different positions for chlorine substitutions (o/p-substitution), they exhibited different cytotoxicity against the two tested cell lines. This may be due to the relevance of chlorine substitution to interact with the corresponding amino acids in the effective target binding site, which will affect the stability of
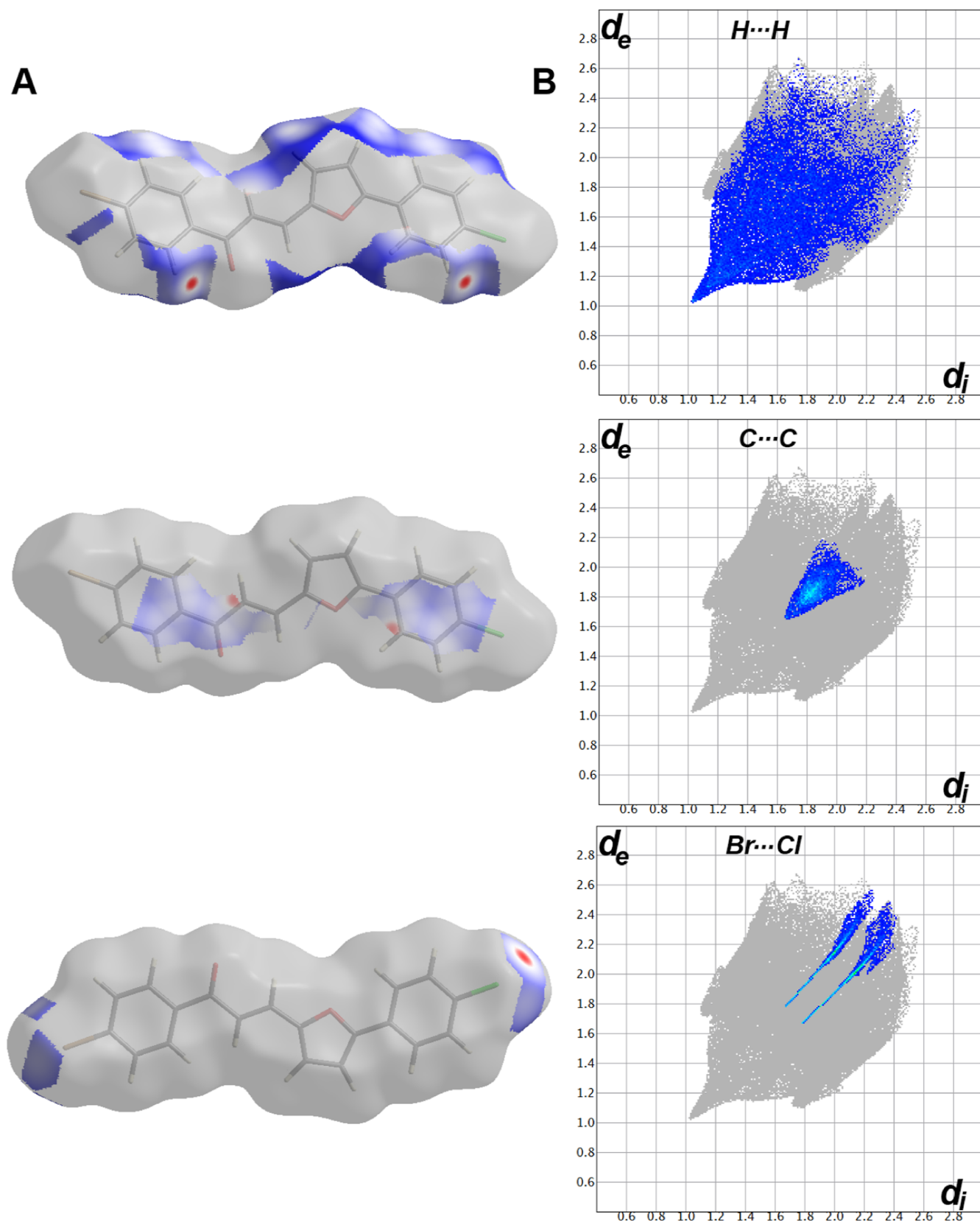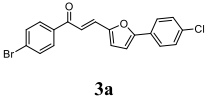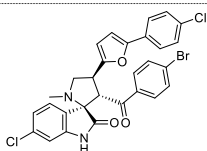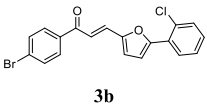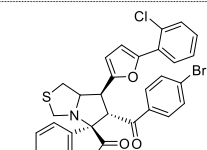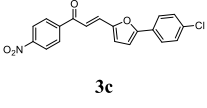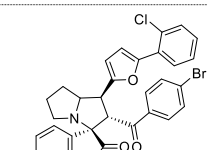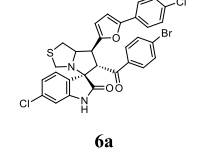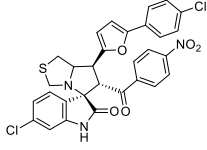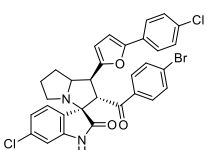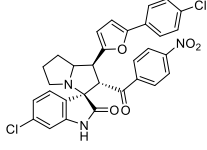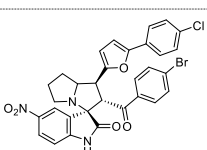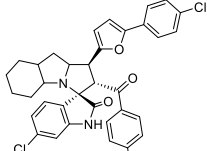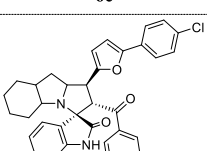
Figure 7. Decomposed d_{norm} maps (A) and fingerprint plots (B) of short contacts in **3a**.

drug–target complexes and the ability of the complex to have a biological response.

For the synthesized spirooxindoles, for the breast cancer cell line (MCF7), spirooxindole having the bulky fused with the

pyrrolidine ring **6d** exhibited the most active hybrid between these series with $IC_{50} = 4.3 \pm 0.18$ μM/mL more potent with 4 folds and the standard staurosporine ($IC_{50} = 17.8 \pm 0.50$ μM/ mL). Next in the reactivity towards cytotoxicity was compound

Table 4. Cytotoxicity Results of the Ethylene Derivatives Having the Aryl-Furan Moiety and the Spirooxindoles against Breast and Liver Carcinoma

≠	Chemical Structure	Cytotoxicity_IC$_{50}$ (μM/mL)[a]	
		MCF-7	HepG2
1	3a	45.9±1.08	59.3±1.12
2	3b	4.1±0.1	3.5±0.07
3	3c	81.3±1.74	36.9±0.64
4	6a	63.1±2.45	91.4±2.86
5	6b	18.2±0.69	27.6±0.84
6	6c	36.7±1.41	45.0±1.39
7	6d	4.3±0.18	6.9±0.23
8	6e	41.2±1.49	25.4±0.74
9	6f	10.33±0.40	3.5±0.11
10	6g	60.5±2.28	36.1±1.10
11	6h	174.3±6.41	54.6±1.62
12	6i	10.7±0.38	19.6±0.56
13	6j	4.7±0.18	11.8±0.37
STD	Staurosporine	17.8±0.50	10.3±0.23

[a]IC$_{50}$ values are expressed as mean ± SD of three independent trials.

spirooxindole **6j** which instead of the Br-atom on the benzoyl ring in compound **6d** replaced by more electron withdrawing group, the reactivity slightly decreased which the IC$_{50}$ equal to 4.7 ± 0.18 μM/mL. Compounds **6f** (IC$_{50}$ = 10.3 ± 0.40 μM/mL) and **6i** (IC$_{50}$ = 10.7 ± 0.38 μM/mL) still provided better cytotoxicity compared to staurosporine. The remaining spirooxindoles provided moderate toxicity against breast adenocarcinoma. Spirooxindoles **6f** (IC$_{50}$ = 3.5 ± 0.11 μM/mL) and **6d** (IC$_{50}$ = 6.9 ± 0.23 μM/mL) were the most active hybrids against human liver cancer cell line (HepG2)

compared to staurosporine [IC$_{50}$ = 10.3 ± 0.23 μM/mL (HepG2)]. The remaining spirooxindoles provided moderate toxicity, and the IC$_{50}$ ranged from 11.8 ± 0.37 to 91.4 ± 2.86 μM/mL.

2.5. Molecular Docking Study. As cyclic-dependent kinase (CDK-2) and epidermal growth factor receptor (EGFR) are key proteins that mediate and trigger the proliferation of cancer cells, their inhibition is an interesting target for apoptosis induction upon treatment of a chemotherapeutic drug.[34−36] A molecular docking study was

performed to highlight the virtual mechanism of binding toward EGFR and CDK-2 proteins. As seen in Figure 8,
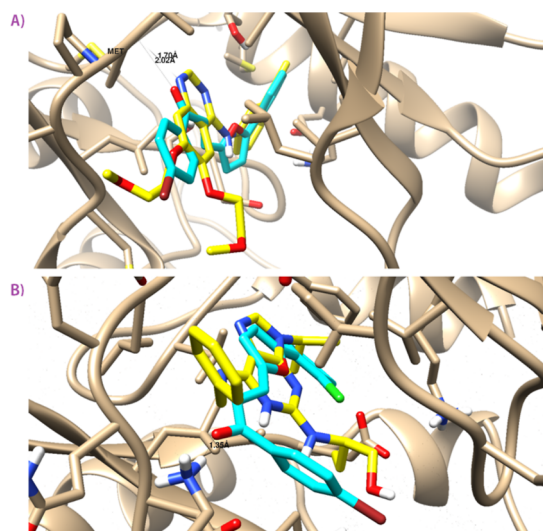

Figure 8. Binding disposition and ligand−receptor interactions of compound **3b** inside the EGFR (A) and CDK-2 (B) proteins. Three-dimensional images were generated by Chimera-UCSF. Cocrystallized ligand (yellow-colored) and docked compound (cyan-colored).

compound **3b** was docked inside the EGFR binding site with the binding energy of −19.63 kcal/mol, and it formed one H-bind interaction with Met 769 as the H-bond acceptor. Additionally, compound **3b** was docked inside the CDK-2 active site with the binding energy of −18.6 Kcal/mol, and it formed one H-bond with Lys 89. Hence, compound **3b** had a good binding affinity toward EGFR and CDK-2 proteins, and these targets may be the effective target for its cytotoxic activity.

3. CONCLUSIONS

We concluded that a set of spirooxindoles having aryl-furan moiety have been successfully synthesized and assessed against two cancer cell lines. The results provided promising data for breast adenocarcinoma and could be utilized as a lead compound for further development. Structural analysis of the newly synthesized compound was performed with the aid of X-ray single crystal structure and Hirshfeld calculations. The reported X-ray structure of **3a** agreed very well with its spectral characterizations. Its supramolecular structure is controlled by many intermolecular contacts such as O···H, H···H, and C···C intermolecular contacts as well as the Br···Cl interhalogen interactions. All intermolecular contacts occurring in the crystal are quantitatively analyzed based on Hirshfeld calculations. The percentages of these contacts are 10.6, 25.7, 6.4, and 6.2%. The biological activity concluded that the new chalcone **3b** showed excellent activity in both MCF7 and HepG2 with IC_{50} = 4.1 ± 0.1 μM/mL (MCF7) and 3.5 ± 0.07 μM/mL (HepG2) compared to staurosporine with 4.3 and 2.92 folds. The synthesized spirooxindole compounds **6d** (IC_{50} = 4.3 ± 0.18 μM/mL), **6f** (IC_{50} = 10.3 ± 0.40 μM/mL), **6i** (IC_{50} = 10.7 ± 0.38 μM/mL), and **6j** (IC_{50} = 4.7 ± 0.18 μM/mL) show high antiproliferative activity *in vitro* against breast adenocarcinoma. On the other hand, compounds **6d** (IC_{50} = 6.9 ± 0.23 μM/mL) and **6f** (IC_{50} = 3.5 ± 0.11 μM/mL) were the most active hybrids against human liver cancer cell line

(HepG2) compared to staurosporine [IC_{50} = 17.8 ± 0.50 μM/mL (MCF7) and 10.3 ± 0.23 μM/mL (HepG2)]. These compounds could be useful for further cancer research development.

4. MATERIALS AND METHODS

All technical instruments and chemicals used in this study are provided in the Supporting Information.

4.1. General Procedure for the Synthesis of the Chalcones (Ethylene Derivatives 3a−c). The synthesis of ethylene derivatives **3a−c** was performed according to the reported procedure by mixing equimolar of the acetophenone derivatives **1a,b** [1-(4-bromophenyl)ethan-1-one **1a**; 1-(4-nitrophenyl)ethan-1-one **1b**] with the corresponding aldehydes **2a,b** [5-(4-chlorophenyl)furan-2-carbaldehyde **2a**; 5-(2-chlorophenyl)furan-2-carbaldehyde **2b**] in the presence of basic condition (NaOH, 2 equiv) in ethanolic solution to give the corresponding ethylene derivatives in a precipitated form which were used for the next step without any further purification.

4.1.1. (E)-1-(4-Bromophenyl)-3-(5-(4-chlorophenyl)furan-2-yl)prop-2-en-1-one 3a. ^{1}H NMR (400 MHz, CDCl$_3$): δ 7.89 (d, J = 8.5 Hz, 2H), 7.71−7.53 (m, 5H), 7.42−7.35 (m, 3H), 6.83−6.72 (m, 2H); ^{13}C NMR (101 MHz, CDCl$_3$): δ 188.59, 155.58, 155.54, 151.39, 151.35, 151.29, 137.04, 134.59, 133.25, 132.10, 132.05, 131.60, 130.89, 130.76, 130.61, 130.56, 129.50, 128.80, 128.33, 128.28, 128.23, 128.04, 127.96, 127.88, 127.04, 125.99, 125.95, 125.64, 124.57, 120.73, 119.83, 118.91, 117.95, 117.04, 110.08, 109.20; chemical formula: C$_{19}$H$_{12}$BrClO$_2$; elemental analysis: C, 58.87; H, 3.12; Found: C, 58.89; H, 3.14.

4.1.2. (E)-1-(4-Bromophenyl)-3-(5-(2-chlorophenyl)furan-2-yl)prop-2-en-1-one 3b. ^{1}H NMR (400 MHz, CDCl$_3$): δ 7.96 (t, J = 7.6 Hz, 1H), 7.91 (t, J = 7.8 Hz, 2H), 7.69−7.56 (m, 3H), 7.52−7.40 (m, 2H), 7.37 (t, J = 7.6 Hz, 1H), 7.33−7.22 (m, 2H), 6.86 (dd, J = 7.3, 3.8 Hz, 1H); ^{13}C NMR (101 MHz, CDCl$_3$): δ 188.68, 152.83, 150.89, 137.03, 132.11, 132.06, 131.95, 131.07, 131.01, 130.87, 130.57, 129.58, 129.03, 128.85, 128.36, 127.97, 127.91, 127.56, 126.76, 119.43, 118.62, 114.57, 113.49; chemical formula: C$_{19}$H$_{12}$BrClO$_2$; elemental analysis: C, 58.87; H, 3.12; Found: C, 58.90; H, 3.15.

4.1.3. (E)-3-(5-(4-Chlorophenyl)furan-2-yl)-1-(4-nitrophenyl)prop-2-en-1-one 3c. ^{1}H NMR (400 MHz, chloroform-D): δ 8.34 (d, J = 8.4 Hz, 2H), 8.16 (d, J = 8.3 Hz, 2H), 7.70 (d, J = 8.3 Hz, 2H), 7.63 (d, J = 15.0 Hz, 1H), 7.42 (t, J = 10.2 Hz, 3H), 6.88 (s, 1H), 6.80 (s, 1H). ^{13}C NMR (101 MHz, chloroform-D): δ 188.18, 156.13, 151.06, 150.14, 143.22, 134.90, 131.88, 129.41, 129.33, 128.12, 125.93, 123.96, 109.03; chemical formula: C$_{19}$H$_{12}$ClNO$_4$; elemental analysis: C, 64.51; H, 3.42; N, 3.96; Found: C, 64.50; H, 3.41; N, 4.00.

4.2. General Method for the Synthesis of the Spirooxindoles Scaffold 6a−j. An equimolar (0.5 mmol) of the ethylene derivatives **3a−c** with isatin derivatives **4a,b** and amino acids **5a−d** in methanol was heated under reflux for 5 h to provide the final products **6a−j** as solid materials in almost quantitative yield upon slow evaporation overnight. In the case of compound **6b**, the crystal quality was not good enough to solve the X-ray structure in a suitable form enough for publication quality but at least provided a reasonable structure for the spiro-compound.

4.2.1. (3R,6′S,7′S)-6′-(4-Bromobenzoyl)-6-chloro-7′-(5-(4-chlorophenyl)furan-2-yl)-1′,6′,7′,7a′-tetrahydro-3′H-spiro-[indoline-3,5′-pyrrolo[1,2-c]thiazol]-2-one 6a. ^{1}H NMR

(400 MHz, CDCl$_3$): δ 8.43 (s, 1H), 7.51 (t, J = 9.1 Hz, 3H), 7.45−7.22 (m, 7H), 7.02 (d, J = 8.1 Hz, 1H), 6.67 (s, 1H), 6.52 (d, J = 3.5 Hz, 1H), 6.32 (d, J = 3.5 Hz, 1H), 4.81 (d, J = 11.7 Hz, 1H), 4.52 (dt, J = 8.9, 4.1 Hz, 1H), 4.15−4.03 (m, 1H), 3.88 (d, J = 11.0 Hz, 1H), 3.46 (d, J = 11.0 Hz, 1H), 3.20 (d, J = 3.9 Hz, 2H). ^{13}C NMR (101 MHz, CDCl$_3$): δ 194.82, 179.72, 152.73, 151.47, 141.76, 136.28, 135.26, 133.13, 132.03, 131.90, 131.75, 130.15, 129.89, 129.71, 129.57, 129.45, 129.09, 129.01, 128.89, 125.07, 124.84, 122.89, 122.65, 120.91, 111.06, 110.78, 106.60, 106.26, 74.31, 72.00, 58.69, 56.40, 45.33, 37.09; IR (KBr, cm^{-1}): 3425, 3310, 2935, 2840, 1720, 1610, 1500; chemical formula: C$_{30}$H$_{21}$BrCl$_2$N$_2$O$_3$S; elemental analysis: C, 56.27; H, 3.31; N, 4.37; S, 5.01; Found: C, 56.17; H, 3.35; N, 4.45; S, 5.09.

4.2.2. (1′S,2′S,3R)-2′-(4-Bromobenzoyl)-6-chloro-1′-(5-(4-chlorophenyl)furan-2-yl)-1′,2′,5′,6′,7′,7a′-hexahydrospiro-[indoline-3,3′-pyrrolizin]-2-one 6b. ^{1}H NMR (400 MHz, CDCl$_3$): δ 8.58 (s, 1H), 7.47 (d, J = 8.6 Hz, 2H), 7.41 (s, 4H), 7.32−7.23 (m, 2H), 7.12 (d, J = 8.1 Hz, 1H), 6.99 (dd, J = 8.0, 2.1 Hz, 1H), 6.77−6.72 (m, 1H), 6.51 (d, J = 3.5 Hz, 1H), 6.26 (d, J = 3.2 Hz, 1H), 4.95 (d, J = 11.6 Hz, 1H), 4.46 (s, 1H), 4.08 (t, J = 10.6 Hz, 1H), 2.73 (d, J = 12.4 Hz, 2H), 2.23 (dt, J = 13.1, 6.7 Hz, 1H), 1.98 (h, J = 6.6, 6.0 Hz, 2H), 1.90 (dd, J = 12.9, 6.6 Hz, 1H); ^{13}C NMR (101 MHz, CDCl$_3$): δ 195.27, 170.74, 152.47, 142.24, 136.10, 135.26, 132.95, 131.67, 129.34, 129.19, 129.09, 128.48, 128.07, 124.63, 123.36, 122.02, 121.86, 114.28, 109.15, 108.99, 108.06, 106.10, 73.42, 67.22, 46.85, 19.53; IR (KBr, cm^{-1}): 3422, 3318, 2930, 2850, 1725, 1610, 1500; chemical formula: C$_{31}$H$_{23}$BrCl$_2$N$_2$O$_3$; elemental analysis: C, 59.83; H, 3.73; N, 4.50; Found: C, 59.79; H, 3.75; N, 4.61.

4.2.3. (1′S,2′S,3R)-2′-(4-Bromobenzoyl)-1′-(5-(4-chlorophenyl)furan-2-yl)-5-nitro-1′,2′,5′,6′,7′,7a′-hexahydrospiro[indoline-3,3′-pyrrolizin]-2-one 6c. ^{1}H NMR (400 MHz, CDCl$_3$): δ 8.96 (s, 1H), 8.23−8.05 (m, 2H), 7.57−7.34 (m, 7H), 7.27 (d, J = 8.1 Hz, 3H), 6.83 (d, J = 8.7 Hz, 1H), 6.51 (d, J = 3.5 Hz, 1H), 6.27 (d, J = 3.5 Hz, 1H), 5.01 (d, J = 11.6 Hz, 1H), 4.39 (dt, J = 12.2, 6.4 Hz, 1H), 4.12 (dd, J = 14.2, 8.3 Hz, 2H), 2.66 (p, J = 6.9, 5.9 Hz, 2H), 2.21 (dt, J = 12.4, 6.5 Hz, 1H), 2.08−1.81 (m, 5H), 1.24 (t, J = 7.0 Hz, 1H); ^{13}C NMR (101 MHz, CDCl$_3$): δ 194.94, 180.62, 171.49, 152.46, 151.98, 146.37, 143.36, 135.20, 132.99, 132.07, 129.61, 129.24, 129.16, 128.94, 126.83, 125.77, 124.85, 123.40, 110.44, 109.24, 106.40, 73.16, 69.08, 61.38, 60.60, 48.25, 46.67, 30.82, 27.62, 14.28.; IR (KBr, cm^{-1}): 3434, 3325, 2922, 2850, 1715, 1608, 1512; chemical formula: C$_{31}$H$_{23}$BrClN$_3$O$_5$; elemental analysis: C, 58.83; H, 3.66; N, 6.64; Found: C, 58.85; H, 3.69; N, 6.71.

4.2.4. (1′S,2′S,3R)-2′-(4-Bromobenzoyl)-6-chloro-1′-(5-(4-chlorophenyl)furan-2-yl)-1′,2′,4a′,5′,6′,7′,8′,8a′,9′,9a′-decahydrospiro[indoline-3,3′-pyrrolo[1,2-a]indol]-2-one 6d. ^{1}H NMR (400 MHz, CDCl$_3$): δ 8.09 (s, 1H), 7.51−7.35 (m, 6H), 7.31−7.23 (m, 2H), 7.14 (d, J = 8.0 Hz, 1H), 7.01 (dd, J = 8.0, 1.7 Hz, 1H), 6.63 (s, 1H), 6.49 (d, J = 3.6 Hz, 1H), 6.20 (d, J = 3.6 Hz, 1H), 5.01 (d, J = 11.8 Hz, 1H), 4.48 (d, J = 8.6 Hz, 1H), 4.00 (t, J = 11.0 Hz, 1H), 3.10 (d, J = 4.3 Hz, 1H), 2.23−2.09 (m, 1H), 2.16 (s, 1H), 1.94 (dd, J = 12.4, 6.4 Hz, 1H), 1.81 (ddd, J = 11.9, 8.5, 6.1 Hz, 1H), 1.60−1.43 (m, 3H), 1.38 (t, J = 12.5 Hz, 1H), 1.17−0.82 (m, 5H); ^{13}C NMR (101 MHz, CDCl$_3$): δ 195.28, 179.74, 178.80, 171.53, 152.56, 152.16, 141.51, 135.49, 132.80, 132.14, 131.58, 129.35, 129.30, 129.26, 128.82, 128.44, 124.62, 122.78, 121.78, 110.95, 108.21, 106.11, 106.07, 71.84, 47.83, 40.45, 34.69, 29.40, 28.77; IR

(KBr, cm^{-1}): 3420, 3317, 2919, 2823, 1715, 1600, 1515; chemical formula: C$_{35}$H$_{29}$BrCl$_2$N$_2$O$_3$; elemental analysis: C, 62.15; H, 4.32; N, 4.14; Found: C, 62.19; H, 4.27; N, 4.06.

4.2.5. (3R,3′S,4′S)-3′-(4-Bromobenzoyl)-6-chloro-4′-(5-(4-chlorophenyl)furan-2-yl)-1′-methylspiro[indoline-3,2′-pyrrolidin]-2-one 6e. ^{1}H NMR (400 MHz, CDCl$_3$): δ 8.42 (s, 1H), 7.46 (d, J = 8.4 Hz, 2H), 7.36 (s, 4H), 7.34 (d, J = 5.4 Hz, 1H), 7.26 (d, J = 7.6 Hz, 3H), 7.04 (d, J = 8.0 Hz, 1H), 6.92 (dd, J = 8.1, 2.1 Hz, 1H), 6.58 (d, J = 2.0 Hz, 1H), 6.51 (d, J = 3.4 Hz, 1H), 6.25 (d, J = 3.4 Hz, 1H), 4.59 (d, J = 6.4 Hz, 2H), 3.74−3.64 (m, 1H), 3.51−3.43 (m, 1H); ^{13}C NMR (101 MHz, CDCl$_3$): δ 195.96, 178.40, 170.35, 152.11, 141.68, 135.67, 135.31, 132.79, 131.83, 131.40, 129.30, 128.91, 128.62, 124.81, 110.18, 106.10, 72.91, 59.96, 57.51, 43.06; IR (KBr, cm^{-1}): 3434, 3320, 2930, 2834, 1725, 1620, 1520; chemical formula: C$_{29}$H$_{21}$BrCl$_2$N$_2$O$_3$; elemental analysis: C, 58.41; H, 3.55; N, 4.70; Found: C, 58.47; H, 3.61; N, 4.79.

4.2.6. (3R,6′S,7′S)-6′-(4-Bromobenzoyl)-6-chloro-7′-(5-(2-chlorophenyl)furan-2-yl)-1′,6′,7′,7a′-tetrahydro-3′H-spiro-[indoline-3,5′-pyrrolo[1,2-c]thiazol]-2-one 6f. ^{1}H NMR (400 MHz, CDCl$_3$): δ 8.17 (s, 1H), 7.74 (d, J = 7.8 Hz, 1H), 7.54 (d, J = 8.1 Hz, 1H), 7.42−7.23 (m, 7H), 7.17 (d, J = 7.5 Hz, 1H), 7.06−6.97 (m, 2H), 6.65 (s, 1H), 6.37 (d, J = 3.2 Hz, 1H), 4.84 (d, J = 11.7 Hz, 1H), 4.51 (td, J = 6.8, 5.4, 3.5 Hz, 1H), 4.14−4.04 (m, 1H), 3.88 (d, J = 10.9 Hz, 1H), 3.50−3.41 (m, 1H), 3.21 (d, J = 5.4 Hz, 2H); ^{13}C NMR (101 MHz, CDCl$_3$): δ 194.84, 179.81, 151.35, 150.04, 141.60, 136.19, 135.31, 131.87, 130.85, 130.09, 129.60, 128.96, 128.20, 127.84, 126.97, 122.77, 121.06, 111.86, 110.78, 109.73, 74.28, 71.82, 59.16, 55.27, 45.29, 37.19, 31.69, 22.75, 14.24; IR (KBr, cm^{-1}): 3428, 3318, 2925, 2840, 1722, 1618, 1508; chemical formula: C$_{30}$H$_{21}$BrCl$_2$N$_2$O$_3$S; elemental analysis: C, 56.27; H, 3.31; N, 4.37; S, 5.01; Found: C, 56.35; H, 3.29; N, 4.41; S, 5.00.

4.2.7. (1′S,2′S,3R)-2′-(4-Bromobenzoyl)-6-chloro-1′-(5-(2-chlorophenyl)furan-2-yl)-1′,2′,5′,6′,7′,7a′-hexahydrospiro-[indoline-3,3′-pyrrolizin]-2-one 6g. ^{1}H NMR (400 MHz, CDCl$_3$): δ 8.69 (s, 1H), 7.70 (d, J = 7.4 Hz, 1H), 7.37 (d, J = 7.7 Hz, 2H), 7.28−7.19 (m, 1H), 7.13 (dd, J = 8.0, 5.2 Hz, 2H), 7.03−6.97 (m, 3H), 6.72 (s, 1H), 6.30 (d, J = 3.1 Hz, 1H), 4.97 (d, J = 11.2 Hz, 1H), 4.36 (dt, J = 9.8, 6.0 Hz, 1H), 4.06 (t, J = 10.6 Hz, 1H), 2.63 (t, J = 6.4 Hz, 2H), 2.18 (dd, J = 12.1, 6.2 Hz, 1H), 1.99−1.80 (m, 4H).; ^{13}C NMR (101 MHz, CDCl$_3$): δ 195.50, 180.56, 152.39, 149.62, 141.93, 135.69, 135.40, 131.88, 130.77, 129.89, 129.66, 129.07, 128.89, 128.59, 127.94, 127.71, 126.92, 123.05, 122.59, 111.87, 111.24, 108.86, 73.20, 68.98, 61.33, 48.25, 46.51, 31.68, 30.94, 27.37, 22.75, 14.23; IR (KBr, cm^{-1}): 3430, 3309, 2918, 2827, 1716, 1608, 1508; chemical formula: C$_{31}$H$_{23}$BrCl$_2$N$_2$O$_3$; elemental analysis: C, 59.83; H, 3.73; N, 4.50; Found: C, 59.80; H, 3.75; N, 4.55.

4.2.8. (3R,6′S,7′S)-6-Chloro-7′-(5-(4-chlorophenyl)furan-2-yl)-6′-(4-nitrobenzoyl)-1′,6′,7′,7a′-tetrahydro-3′H-spiro-[indoline-3,5′-pyrrolo[1,2-c]thiazol]-2-one 6h. ^{1}H NMR (400 MHz, CDCl$_3$): δ 8.38 (s, 1H), 8.08 (d, J = 8.6 Hz, 2H), 7.54 (dd, J = 17.7, 8.6 Hz, 5H), 7.30 (d, J = 8.2 Hz, 2H), 7.04 (dd, J = 8.1, 2.1 Hz, 1H), 6.65 (d, J = 1.8 Hz, 1H), 6.54 (d, J = 3.1 Hz, 1H), 6.38 (d, J = 3.6 Hz, 1H), 4.85 (d, J = 11.7 Hz, 1H), 4.53 (dt, J = 9.7, 3.9 Hz, 1H), 4.15−4.00 (m, 1H), 3.88 (d, J = 11.1 Hz, 1H), 3.46 (d, J = 11.1 Hz, 1H), 3.20 (d, J = 3.9 Hz, 2H); ^{13}C NMR (101 MHz, CDCl$_3$): δ 194.92, 179.53, 152.88, 151.11, 150.38, 141.79, 141.08, 136.60, 133.25, 131.08, 129.93, 129.18, 129.07, 129.04, 129.01, 128.94, 124.96, 123.69, 123.57, 122.96, 120.70, 110.18, 106.47, 74.11, 71.71,

60.61, 59.94, 55.31, 45.22, 37.09, 14.28; IR (KBr, cm^{-1}): 3422, 3320, 2920, 2850, 1730, 1620, 1511; chemical formula: $C_{30}H_{21}Cl_2N_3O_5S$; elemental analysis: C, 59.41; H, 3.49; N, 6.93; S, 5.29; Found: C, 59.44; H, 3.51; N, 7.02; S, 5.36.

4.2.9. (1′S,2′S,3R)-6-Chloro-1′-(5-(4-chlorophenyl)furan-2-yl)-2′-(4-nitrobenzoyl)-1′,2′,5′,6′,7′,7a′-hexahydrospiro-[indoline-3,3′-pyrrolizin]-2-one 6i. ^{1}H NMR (400 MHz, CDCl$_3$): δ 8.92 (s, 1H), 8.36 (d, *J* = 8.3 Hz, 1H), 8.23 (d, *J* = 8.7 Hz, 1H), 8.05 (d, *J* = 8.6 Hz, 2H), 7.60 (d, *J* = 8.2 Hz, 2H), 7.46 (d, *J* = 8.6 Hz, 2H), 7.46 (s, 0H), 7.26 (d, *J* = 8.2 Hz, 2H), 7.12 (d, *J* = 11.9 Hz, 1H), 7.02 (d, *J* = 8.2 Hz, 1H), 6.68 (s, 1H), 6.51 (d, *J* = 3.0 Hz, 1H), 6.28 (d, *J* = 3.5 Hz, 1H), 4.98 (d, *J* = 11.6 Hz, 1H), 4.32 (dt, *J* = 9.9, 6.3 Hz, 1H), 4.15−3.96 (m, 1H), 2.57 (dt, *J* = 6.6, 4.2 Hz, 2H), 2.15 (dt, *J* = 12.8, 6.3 Hz, 1H), 1.90 (p, *J* = 6.4 Hz, 2H), 1.82 (dt, *J* = 13.5, 6.3 Hz, 1H); ^{13}C NMR (101 MHz, CDCl$_3$): δ 195.56, 180.70, 171.46, 152.40, 150.76, 150.34, 142.00, 141.20, 140.87, 135.93, 132.95, 129.73, 129.18, 129.08, 129.02, 128.95, 128.89, 128.85, 128.41, 127.43, 124.83, 124.61, 124.34, 124.05, 123.69, 123.34, 122.96, 122.76, 111.36, 109.52, 109.12, 108.76, 106.40, 106.17, 73.18, 69.02, 64.69, 62.38, 60.58, 48.14, 46.41, 31.02, 27.42, 14.27; IR (KBr, cm^{-1}): 3423, 3317, 2935, 2845, 1723, 1606, 1516; chemical formula: $C_{31}H_{23}Cl_2N_3O_5$; elemental analysis: C, 63.28; H, 3.94; N, 7.14; Found: C, 63.34; H, 3.99; N, 7.24.

4.2.10. (1′S,2′S,3R)-6-chloro-1′-(5-(4-chlorophenyl)furan-2-yl)-2′-(4-nitrobenzoyl)-1′,2′,4a′,5′,6′,7′,8′,8a′,9′,9a′-decahydrospiro[indoline-3,3′-pyrrolo[1,2-a]indol]-2-one 6j. ^{1}H NMR (400 MHz, CDCl$_3$): δ 8.12 (d, *J* = 8.7 Hz, 3H), 7.59 (d, *J* = 8.7 Hz, 2H), 7.49 (d, *J* = 8.2 Hz, 2H), 7.28 (d, *J* = 8.1 Hz, 2H), 7.13 (d, *J* = 8.0 Hz, 1H), 7.04 (d, *J* = 8.5 Hz, 1H), 6.61 (s, 1H), 6.51 (d, *J* = 3.6 Hz, 1H), 6.26 (d, *J* = 3.6 Hz, 1H), 5.05 (d, *J* = 11.7 Hz, 1H), 4.48 (q, *J* = 8.3, 7.5 Hz, 1H), 3.98 (t, *J* = 10.9 Hz, 1H), 3.12−3.05 (m, 1H), 2.17 (dq, *J* = 9.9, 4.8 Hz, 1H), 1.97−1.89 (m, 1H), 1.81 (dt, *J* = 13.7, 6.3 Hz, 1H), 1.52 (q, *J* = 14.4 Hz, 3H), 1.36 (q, *J* = 12.6 Hz, 1H), 1.02 (dddd, *J* = 48.7, 25.8, 9.8, 3.6 Hz, 3H), 0.84 (d, *J* = 14.7 Hz, 1H); ^{13}C NMR (101 MHz, CDCl$_3$): δ 195.39, 181.09, 174.14, 152.31, 152.24, 150.37, 141.50, 141.35, 135.69, 132.93, 129.21, 129.15, 128.93, 128.85, 124.86, 123.68, 122.49, 122.16, 111.04, 109.01, 106.38, 71.61, 68.01, 63.26, 60.57, 57.93, 53.55, 47.20, 41.75, 37.62, 28.32, 27.59, 24.52, 19.92, 14.27; IR (KBr, cm^{-1}): 3429, 3314, 2927, 2837, 1720, 1610, 1505; chemical formula: $C_{35}H_{29}Cl_2N_3O_5$; elemental analysis: C, 65.43; H, 4.55; N, 6.54; Found: C, 65.45; H, 4.54; N, 6.64.

4.3. X-ray Structure Determinations. The crystal of **3a** was immersed in cryo-oil, mounted in a loop, and measured at a temperature of 120 K. The X-ray diffraction data were collected on a Rigaku Oxford Diffraction Supernova diffractometer using Mo Kα radiation. The CrysAlisPro[37] software package was used for cell refinement and data reduction. An analytical absorption correction (CrysAlisPro[37]) was applied to the intensities before structure solution. The structure was solved by intrinsic phasing (SHELXT[38]) method. Structural refinement was carried out using SHELXL[39] software with the SHELXLE[40] graphical user interface. Hydrogen atoms were positioned geometrically and constrained to ride on their parent atoms, with C−H = 0.95 Å and U_{iso} = 1.2U_{eq} (parent atom).

4.4. Hirshfeld Surface Analysis. Crystal Explorer 17.5 program[41] was used to perform the Hirshfeld topology analysis.

4.5. Molecular Docking Study. The investigated compounds were docked against the protein structures of EGFR (PDB = 1M17) and CDK-2 (PDB = 2A4L) using AutoDock Vina software following routine work.[42−45] Vina was used to improve protein and ligand structures and favor them energetically. Proteins and compound structures were prepared and optimized using Maestro. Then, the binding sites inside proteins were determined using grid-box dimensions around the cocrystallized ligands. Binding activities interpreted molecular docking results in terms of binding energy and ligand−receptor interactions. The visualization was then done with Chimera.

■ ASSOCIATED CONTENT

Ⓢ Supporting Information

The Supporting Information is available free of charge at https://pubs.acs.org/doi/10.1021/acsomega.2c03790.

Crystallized copmound (CIF)

MTT assay and ^{1}HNMR and ^{13}CNMR of the synthesized compounds **3a−c** and **6a−j** (PDF)

■ AUTHOR INFORMATION

Corresponding Authors

Mezna Saleh Altowyan − *Department of Chemistry, College of Science, Princess Nourah bint Abdulrahman University, Riyadh 11671, Saudi Arabia*; Email: msaltowyan@pnu.edu.sa

Assem Barakat − *Department of Chemistry, College of Science, King Saud University, Riyadh 11451, Saudi Arabia*; ⓘ orcid.org/0000-0002-7885-3201; Email: ambarakat@ksu.edu.sa

Authors

Saied M. Soliman − *Department of Chemistry, Faculty of Science, Alexandria University, Alexandria 21321, Egypt*; ⓘ orcid.org/0000-0001-8405-8370

Matti Haukka − *Department of Chemistry, University of Jyväskylä, Jyväskylä FI-40014, Finland*; ⓘ orcid.org/0000-0002-6744-7208

Nora Hamad Al-Shaalan − *Department of Chemistry, College of Science, Princess Nourah bint Abdulrahman University, Riyadh 11671, Saudi Arabia*; ⓘ orcid.org/0000-0002-5285-2155

Aminah A. Alkharboush − *Department of Chemistry, College of Science, Princess Nourah bint Abdulrahman University, Riyadh 11671, Saudi Arabia*

Complete contact information is available at:
https://pubs.acs.org/10.1021/acsomega.2c03790

Author Contributions

Conceptualization, A.B.; methodology, M.S.A. and A.A.A.; software, S.M.S. and M.H.; validation, M.S.A., N.H.A.-S., and A.A.A.; formal analysis, M.S.A., N.H.A.-S., M.H., and A.A.A.; investigation, M.S.A.; resources, M.S.A. and A.B.; data curation, A.B. and S.M.S.; writing—original draft preparation, A.B. and S.M.S.; writing—review and editing, A.B. and S.M.S.; visualization, A.B., M.S.A., and N.H.A.-S.; supervision, A.B. and M.S.A.; project administration, A.A.A.; funding acquisition, M.S.A. All authors have read and agreed to the published version of the manuscript.

Notes

The authors declare no competing financial interest.

■ REFERENCES

(1) Panda, S. S.; Jones, R. A.; Bachawala, P.; Mohapatra, P. P. Spirooxindoles as Potential Pharmacophores. *Mini-Rev. Med. Chem.* **2017**, *17*, 1515−1536.

(2) Zhou, L. M.; Qu, R. Y.; Yang, G. F. An Overview of Spirooxindole as a Promising Scaffold for Novel drug Discovery. *Expert Opin. Drug Discovery* **2020**, *15*, 603−625.

(3) Yu, B.; Yu, D. Q.; Liu, H. M. Spirooxindoles: Promising scaffolds for anticancer agents. *Eur. J. Med. Chem.* **2015**, *97*, 673−698.

(4) Zhao, Y.; Yu, S.; Sun, W.; Liu, L.; Lu, J.; McEachern, D.; Shargary, S.; Bernard, D.; Li, X.; Zhao, T.; Zou, P.; Sun, D.; Wang, S. A Potent Small-Molecule Inhibitor of the MDM2-p53 Interaction (MI-888) Achieved Complete and Durable Tumor Regression in Mice. *J. Med. Chem.* **2013**, *56*, 5553−5561.

(5) Lu, J.; Guan, S.; Zhao, Y.; Yu, Y.; Wang, Y.; Shi, Y.; Mao, X.; Yang, K. L.; Sun, W.; Xu, X.; Yi, J. S.; Yang, T.; Yang, J.; Nuchtern, J. G. Novel MDM2 Inhibitor SAR405838 (MI-773) Induces p53-Mediated Apoptosis in Neuroblastoma. *Oncotarget* **2016**, *7*, 82757.

(6) Zheng, M.; Yang, J.; Xu, X.; Sebolt, J. T.; Wang, S.; Sun, Y. Efficacy of MDM2 Inhibitor MI-219 Against Lung Cancer Cells Alone or in Combination with MDM2 Knockdown, a XIAP Inhibitor or Etoposide. *Anticancer Res.* **2010**, *30*, 3321.

(7) Zhao, B. L.; Du, D. M. Organocatalytic Cascade Michael/Michael Reaction for the Asymmetric Synthesis of Spirooxindoles Containing Five Contiguous Stereocenters. *Chem. Commun.* **2016**, *52*, 6162−6165.

(8) Galliford, C. V.; Scheidt, K. A. Pyrrolidinyl-Spirooxindole Natural Products as Inspirations for the Development of Potential Therapeutic Agents. *Angew. Chem., Int. Ed.* **2007**, *46*, 8748−8758.

(9) Liu, J.; Peng, H.; Yang, Y.; Jiang, H.; Yin, B. Regioselective and Stereoselective Pd-Catalyzed Intramolecular Arylation of Furans: Access to Spirooxindoles and 5H-Furo[2,3-c]quinolin-4-ones. *J. Org. Chem.* **2016**, *81*, 9695−9706.

(10) Pan, L. N.; Sun, J.; Shi, R. G.; Yan, C. G. Diastereoselective synthesis of dispiro[indoline-3,3′-furan-2′,3″-pyrrolidine] via [3 + 2]cycloaddition reaction of MBH maleimides of isatins and 1,3-dicarbonyl compounds. *Org. Chem. Front.* **2020**, *7*, 3202−3208.

(11) Yin, B.-L.; Lai, J. Q.; Zhang, Z. R.; Jiang, H. F. A Novel Entry to Spirofurooxindoles Involving Tandem Dearomatization of Furan Ring and Intramolecular Friedel−Crafts Reaction. *Adv. Synth. Catal.* **2011**, *353*, 1961−1965.

(12) Gupta, N.; Bhojani, G.; Tak, R.; Jakhar, A.; Khan, N. U. H.; Chatterjee, S.; Kureshy, R. I. Highly Diastereoselective Syntheses of Spiro-Oxindole Dihydrofuran Derivatives in Aqueous Media and Their Antibacterial Activity. *ChemistrySelect* **2017**, *2*, 10902−10907.

(13) Liu, Z.; Fang, J.; Yan, C. Efficient Synthesis of Spiro[furan-3,3′-indoline] Derivatives via Reactions of Pyridinium Salts with Isatinylidene Acetoacetates. *Chin. J. Chem.* **2013**, *31*, 1054−1058.

(14) Ball-Jones, N. R.; Badillo, J. J.; Franz, A. K. Strategies for the Enantioselective Synthesis of Spirooxindoles. *Org. Biomol. Chem.* **2012**, *10*, 5165−5181.

(15) Kumarswamyreddy, N.; Kesavan, V. Stereoselective and Regioselective Assembly of Spirooxindole [2,1-b]furan Motifs through a Tandem Friedel-Crafts Alkylation/5-exo-dig-Cyclization. *Eur. J. Org. Chem.* **2016**, 5301−5308.

(16) Kumarswamyreddy, N.; Kesavan, V. Enantioselective Synthesis of Dihydrospiro[indoline-3,4′-pyrano[2,3-c]pyrazole] Derivatives via Michael/Hemiketalization Reaction. *Org. Lett.* **2016**, *18*, 1354−1357.

(17) Xie, X.; Peng, C.; He, G.; Leng, H. J.; Wang, B.; Huang, W.; Han, B. Asymmetric Synthesis of a Structurally and Stereochemically Complex Spirooxindole Pyran Scaffold Through an Organocatalytic Multicomponent Cascade Reaction. *Chem. Commun.* **2012**, *48*, 10487−10489.

(18) Chowdhury, S.; Chafeev, M.; Liu, S.; Sun, J.; Raina, V.; Chui, R.; Young, W.; Kwan, R.; Fu, J.; Cadieux, J. A. Discovery of XEN907, a spirooxindole blocker of NaV1.7 for the treatment of pain. *Bioorg. Med. Chem. Lett.* **2011**, *21*, 3676−3681.

(19) Altowyan, M. S.; Barakat, A.; Al-Majid, A. M.; Al-Ghulikah, H. Spiroindolone analogues bearing benzofuran moiety as a selective cyclooxygenase COX-1 with TNF-α and IL-6 inhibitors. *Saudi J. Biol. Sci.* **2020**, *27*, 1208−1216.

(20) Lotfy, G.; Abdel Aziz, Y. M. A.; Said, M. M.; El Ashry, E. S. H.; El Tamany, E. S. H.; Abu-Serie, M. M.; Teleb, M.; Dömling, A.; Barakat, A. Molecular Hybridization Design and Synthesis of Novel Spirooxindole-Based MDM2 Inhibitors Endowed with BCL2 Signaling Attenuation; A Step Towards the Next Generation p53 Activators. *Bioorg. Chem.* **2021**, *117*, 105427.

(21) Barakat, A.; Islam, M. S.; Ghawas, H. M.; Al-Majid, A. M.; El-Senduny, F.; Badria, F. A.; Elshaier, Y.; Ghabbour, H. A. Design and synthesis of new substituted spirooxindoles as potential inhibitors of the MDM2-p53 interaction. *Bioorg. Chem.* **2019**, *86*, 598−608.

(22) Barakat, A.; Haukka, M.; Soliman, S. M.; Ali, M.; Al-Majid, A. M.; El-Faham, A.; Domingo, L. R. Straightforward Regio- and Diastereoselective Synthesis, Molecular Structure, Intermolecular Interactions and Mechanistic Study of Spirooxindole-Engrafted Rhodanine Analogs. *Molecules* **2021**, *26*, 7276.

(23) Aziz, Y. M. A.; Lotfy, G.; Said, M. M.; El Ashry, E. S. H.; El Tamany, E. S. H.; Soliman, S. M.; Abu-Serie, M. M.; Teleb, M.; Yousuf, S.; Dömling, A.; et al. Design, Synthesis, Chemical and Biochemical Insights into Novel Hybrid Spirooxindole-Based p53-MDM2 Inhibitors with Potential Bcl2 Signaling Attenuation. *Front. Chem.* **2021**, *9*, 735236.

(24) Al-Majid, A. M.; Ali, M.; Islam, M. S.; Alshahrani, S.; Alamary, A. S.; Yousuf, S.; Choudhary, M. I.; Barakat, A. Stereoselective Synthesis of the Di-Spirooxindole Analogs Based Oxindole and Cyclohexanone Moieties as Potential Anticancer Agents. *Molecules* **2021**, *26*, 6305.

(25) Barakat, A.; Islam, M. S.; Ali, M.; Al-Majid, A. M.; Alshahrani, S.; Alamary, A. S.; Yousuf, S.; Choudhary, M. I. Regio- and Stereoselective Synthesis of a New Series of Spirooxindole Pyrrolidine Grafted Thiochromene Scaffolds as Potential Anticancer Agents. *Symmetry* **2021**, *13*, 1426.

(26) Islam, M. S.; Ghawas, H. M.; El-Senduny, F. F.; Al-Majid, A. M.; Elshaier, Y. A.; Badria, F. A.; Barakat, A. Synthesis of new thiazolo-pyrrolidine-(spirooxindole) tethered to 3-acylindole as anticancer agents. *Bioorg. Chem.* **2019**, *82*, 423−430.

(27) Lotfy, G.; Said, M. M.; El Ashry, H.; El Tamany, H.; Al-Dhfyan, A.; Abdel Aziz, Y. M. A.; Barakat, A. Synthesis of New Spirooxindole-Pyrrolothiazole Derivatives: Anti-Cancer Activity and Molecular Docking. *Bioorg. Med. Chem.* **2017**, *25*, 1514−1523.

(28) Barakat, A.; Islam, M. S.; Ghawas, H. M.; Al-Majid, A. M.; El-Senduny, F. F.; Badria, F. A.; Elshaier, Y. A. M.; Ghabbour, H. A. Substituted Spirooxindole Derivatives as Potent antiCancer Agents Through Inhibition of Phosphodiesterase 1. *RSC Adv.* **2018**, *8*, 14335−14346.

(29) Ríos-Gutiérrez, M.; Domingo, L. R. Unravelling the Mysteries of the [3+2] Cycloaddition Reactions. *Eur. J. Org. Chem.* **2019**, 267−282.

(30) Domingo, L. R.; Chamorro, E.; Perez, P. Understanding the High Reactivity of the Azomethine Ylides in [3 + 2] Cycloaddition Reactions. *Lett. Org. Chem.* **2010**, *7*, 432−439.

(31) Domingo, L. R.; Kula, K.; Ríos-Gutiérrez, M. Unveiling the Reactivity of Cyclic Azomethine Ylides in [3+2] Cycloaddition Reactions within the Molecular Electron Density Theory. *Eur. J. Org. Chem.* **2020**, 5938−5948.

(32) Domingo, L. R.; Ríos-Gutiérrez, M.; Pérez, P. A Molecular Electron Density Theory Study of the Role of the Copper Metalation of Azomethine Ylides in [3 + 2] Cycloaddition Reactions. *J. Org. Chem.* **2018**, *83*, 10959−10973.

(33) Ríos-Gutiérrez, M.; Barakat, A.; Domingo, L. R. A Molecular Electron Density Theory Study of the [3+2] Cycloaddition Reaction

of Pseudo(mono)radical Azomethine Ylides with Phenyl Vinyl Sulphone. *Organics* **2022**, *3*, 122−136.

(34) Faber, A. C.; Chiles, T. C. Inhibition of Cyclin-Dependent Kinase-2 Induces Apoptosis in Human Diffuse Large B-Cell Lymphomas. *Cell Cycle* **2007**, *6*, 2982−2989.

(35) ElZahabi, H. S. A.; Nafie, M. S.; Osman, D.; Elghazawy, N. H.; Soliman, D. H.; EL-Helby, A. A. H.; Arafa, R. K. Design, Synthesis and Evaluation of New Quinazolin-4-one Derivatives as Apoptotic Enhancers and Autophagy Inhibitors with Potent Antitumor Activity. *Eur. J. Med. Chem.* **2021**, *222*, 113609.

(36) Nafie, M. S.; Kishk, S. M.; Mahgoub, S.; Amer, A. M. -Quinoline-based thiazolidinone derivatives as potent cytotoxic and apoptosis-inducing agents through EGFR inhibition. *Chem. Biol. Drug Des.* **2022**, *99*, 547−560.

(37) Sheldrick, G. M. *SADABS-Bruker Nonius Scaling and Absorption Correction*; Bruker AXS, Inc.: Madison, Wisconsin, USA, 2012.

(38) Sheldrick, G. M. SHELXT- Integrated space-group and crystal-structure determination. *Acta Crystallogr., Sect. A: Found. Adv.* **2015**, *71*, 3−8.

(39) Sheldrick, G. M. Crystal structure refinement withSHELXL. *Acta Crystallogr., Sect. C: Struct. Chem.* **2015**, *71*, 3−8.

(40) Hübschle, C. B.; Sheldrick, G. M.; Dittrich, B. ShelXle: a Qt Graphical User Interface for SHELXL. *J. Appl. Crystallogr.* **2011**, *44*, 1281−1284.

(41) Turner, M. J.; McKinnon, J. J.; Wolff, S. K.; Grimwood, D. J.; Spackman, P. R.; Jayatilaka, D.; Spackman, M. A. *Crystal Explorer17*; University of Western Australia, 2017. http://hirshfeldsurface.net.

(42) Nafie, M. S.; Tantawy, M. A.; Elmgeed, G. A. Screening of Different Drug Design Tools to Predict the Mode of Action of Steroidal Derivatives as Anti-cancer Agents. *Steroids* **2019**, *152*, 108485.

(43) Nafie, M. S.; Amer, A. M.; Mohamed, A. K.; Tantawy, E. S. Discovery of Novel Pyrazolo[3,4-b]pyridine Scaffold-Based Derivatives as Potential PIM-1 Kinase Inhibitors in Breast Cancer MCF-7 Cells. *Bioorg. Med. Chem.* **2020**, *28*, 115828.

(44) Nafie, M. S.; Arafa, K.; Sedky, N. K.; Alakhdar, A. A.; Arafa, R. K. Triaryl dicationic DNA Minor-Groove Binders with Antioxidant Activity Display Cytotoxicity and Induce Apoptosis in Breast Cancer. *Chem.-Biol. Interact.* **2020**, *324*, 109087.

(45) Khalifa, M. M.; Al-Karmalawy, A. A.; Elkaeed, E. B.; Nafie, M. S.; Tantawy, M. A.; Eissa, I. H.; Mahdy, H. A. Topo II Inhibition and DNA Intercalation by New Phthalazine-Based Derivatives as Potent Anticancer Agents: Design, Synthesis, Anti-Proliferative, Docking, and in vivo Studies. *J. Enzyme Inhib. Med. Chem.* **2022**, *37*, 299−314.